INSTITUTE OF PHYSICS PUBLISHING JOURNAL OF PHYSICS: CONDENSED MATTER

J. Phys.: Condens. Matter **13** (2001) 2677–2689 www.iop.org/Journals/cm PII: S0953-8984(01)18374-8

Polar phonons and central mode in antiferroelectric $PbZrO_3$ ceramics

T Ostapchuk[1], J Petzelt[1], V Zelezny[1], S Kamba[1], V Bovtun[1], V Porokhonskyy[1], A Pashkin[1], P Kuzel[1], M D Glinchuk[2], I P Bykov[2], B Gorshunov[3,4] and M Dressel[3]

[1] Institute of Physics, Academy of Sciences of the Czech Republic, Na Slovance 2, 182 21 Praha 8, Czech Republic
[2] Institute for Problems of Materials Science, NASU, Krjijanovskogo street 3, 03 142 Kiev, Ukraine
[3] Physikalisches Institut, Universität Stuttgart, D-70550 Stuttgart, Germany

Received 27 October 2000, in final form 1 February 2001

Abstract

Infrared reflectivity spectra of lead zirconate ceramics were measured in the frequency region of 20–3000 cm^{-1} and temperature range from 10 to 900 K. The data, extended to lower frequencies by coherent source submillimetre, time-domain terahertz transmission and microwave dielectric spectroscopies, were fitted with the factorized model of the dielectric function. Besides the polar optical phonons, one of which slightly softens in the vicinity of the antiferroelectric phase transition, a central-mode type dispersion was revealed in the 5–25 cm^{-1} (10^{11}–10^{12} Hz) range. This central mode is found to be responsible for the strong dielectric anomaly in the paraelectric phase, whereas the lattice phonon contribution does not exceed $\varepsilon' \sim 300$ in the vicinity of T_c. We attribute the origin of the central mode to the lattice disorder caused by strongly anharmonic hopping of Pb ions.

1. Introduction

Lead zirconate $PbZrO_3$ (PZ) deserves special attention for two main reasons: as the first compound where antiferroelectricity was found and as the end member of the $PbZr_{1-x}Ti_xO_3$ system, which is currently used for many applications. Its cubic perovskite structure (space group O_h^1–$Pm3m$, $Z = 1$) transforms into the orthorhombic one (D_{2h}^9–$Pbam$, $Z = 8$) at $T_c \sim 508$ K undergoing a first order phase transition [1, 2]. In many PZ crystals and ceramics a transient ferroelectric phase of rhombohedral symmetry has been observed in a narrow temperature interval (∼10 K) between antiferro- and paraelectric phases [3, 4]. Its existence seems to be related to the defect concentration and stoichiometry [3–5]. These factors considerably alter the dielectric properties of PZ even far from the phase transition. In table 1 we have collected the values of the dielectric permittivity and loss measured on several PZ

[4] Permanent address: General Physics Institute, RAS, Vavilov Street 38, 117945 Moscow, Russia.

 © 2001 IOP Publishing Ltd Printed in the UK

Table 1. Dielectric characteristics of different PZ samples at selected frequencies. Some values were estimated from figures and the error should be considered in the context of the mentioned papers.

Frequency	Characteristic	PZ crystals [6] (poly- and mono-domain)	PZ ceramics					
			[7]	[8]	[9]	[l0]	[11]	[3]
Room temperature values								
1–100 kHz	ε'		150			160	180	
	$\tan\delta$					0.05		
1 MHz	ε'	175	150	85	85	160		
	$\tan\delta$	<0.01				0.005		
10 MHz	ε'	170				150		
	$\tan\delta$	0.03				0.01		
1 GHz	ε'	30		80		140		
	$\tan\delta$	0.5		0.005		0.03		
37 GHz	ε'			80	80	120		
	$\tan\delta$			0.035	0.03	0.05		
78 GHz	ε'				80			
	$\tan\delta$				0.1			
Maximum values								
1–100 kHz	ε'	4600	4700				6000	3300
	$\tan\delta$							
1 MHz	ε'	4200	4400	2600	2500			
	$\tan\delta$	0.1						
10 MHz	ε'	2000						
	$\tan\delta$	1						
1 GHz	ε'	100						
	$\tan\delta$	0.5						
37 GHz	ε'			2500	2400			
	$\tan\delta$			>0.2	>0.2			
78 GHz	ε'				<1500			
	$\tan\delta$				>0.6			

crystals and ceramics [6–11] for room and Curie temperatures at selected frequencies. In spite of the wide scattering of these data, [8–10] demonstrate the same tendency: throughout the frequency range 1 MHz–78 GHz, the dielectric permittivity slightly decreases and the loss gradually grows with increasing frequency in the antiferroelectric phase. A considerably stronger dielectric dispersion starts in the 10^{10}–10^{11} Hz range above T_c [8, 9]. The dispersion in the permittivity observed in [6] on single crystals was, however, revealed at much lower frequencies (10^6–10^9 Hz) and gave no space for a strong dispersion at higher frequencies.

The mentioned diversity in the dielectric data led to different interpretations of the phase transition dynamics in PZ. Some authors [8, 10] assumed that the observed microwave dispersion is the wing of the infrared (IR) absorption peak corresponding to the low-frequency soft lattice mode. This assumption was based on the Kramers–Kronig analysis of the room temperature IR reflectivity spectra of ceramics [12], which revealed a low-frequency lattice phonon, contributing by about 90% to the static permittivity. Roleder *et al* [6] assigned the observed MHz dispersion to a polar relaxation mode, connecting its existence with the disorder in the Pb sublattice. This suggestion was supported by the fact that no mode softening had been observed in PZ by that time. Indeed, inelastic neutron scattering experiments that would have

been able to give an experimental evidence of the lattice softening are not possible because of small size of available single crystals. The only accessible information can be obtained from optical experiments near the centre of the Brillouin zone. However, no temperature evolution of IR spectra had been measured until our preliminary report [13]. The Raman spectra did not reveal any clear mode softening below T_c [14, 15] and in accordance with the selection rules all Raman modes become inactive in the paraelectric phase.

Recently, an attempt was undertaken to evaluate the paraelectric soft lattice mode from the defect-induced Raman spectra measured on a single crystal [16, 17], but the small observed softening could not explain the $\varepsilon'(T)$ dependence. Considering this fact and assigning the main contribution to the static dielectric permittivity to a strong relaxation in the 10^6–10^9 Hz range, Roleder *et al* [17] concluded that the phase transition in PZ is of the mixed order–disorder and displacive type. Our recent paper [13], where the first IR results on PZ crystal, ceramics and films in a wide temperature range were reported, supported this idea. Our IR spectra also revealed a partial softening of the low-frequency lattice mode, whose contribution to the paraelectric dielectric anomaly was rather small. Besides, a low-frequency increase in the far-IR reflectivity indicated the existence of a central-mode-like excitation at ∼5–25 cm^{-1} (∼10^{11}–10^{12} Hz), i.e. appreciably higher than reported in [6] and [17]. The quantitative evaluation of the mode parameters was performed only for the data measured on a thin single crystalline polydomain platelet. The crystal spectra showed sharper features than those of ceramics, allowing us to resolve more phonons, but it was difficult to avoid ambiguity in distinguishing between phonon reflection peaks and interference fringes in the regions of crystal transparency. Therefore, a detailed analysis of the reflectivity spectra of the thicker opaque ceramics given in the present paper could be very helpful. Moreover, in this work the temperature and frequency ranges of the measurements are extended and different experimental techniques are compared.

2. Experiment

The preparation of the PZ ceramics used in the present work is described in [7]. Its density is ∼98% of the theoretical one and the grain size is of the order of 1 μm. The polished sample of disc shape ($d = 8$ mm, $h = 1$ mm) was used for the IR reflectivity measurements (20–3000 cm^{-1}), performed with the Fourier transform spectrometer Bruker IFS 113v with the resolution of 2 cm^{-1}. The spectrometer was equipped with a room temperature DTGS pyroelectric detector as well as an He-cooled (1.5 K) Si bolometer. A continuous-flow Oxford CF 104 cryostat was used for cooling the sample down to ∼10 K and a home-made furnace for its heating up to 900 K. In order to exclude the distortion of the spectra at higher temperatures due to the thermal emission of the sample, we subtracted the interferograms of the non-illuminated sample (measured with the masked IR source) from the interferograms of the illuminated one [18].

Measurements in the frequency range 10–20 cm^{-1} were performed using a tunable coherent source millimetre-submillimetre spectrometer [19] within the temperature interval 10–300 K. The dielectric spectra were calculated from the complex transmission function of the 43 μm thick plane-parallel sample. The same sample was used for time-domain terahertz transmission measurements whose setup was described elsewhere [20]; the method was used only at room temperature and covered the 5–30 cm^{-1} frequency range. For microwave dielectric measurements performed within 300–500 K at 36 GHz, a rectangular waveguide impedance method was used [21, 22]. The plate-shaped sample (0.3 mm thick), covering the full cross-section (7.112×3.556 mm^2), was inserted into the end of the shorted waveguide.

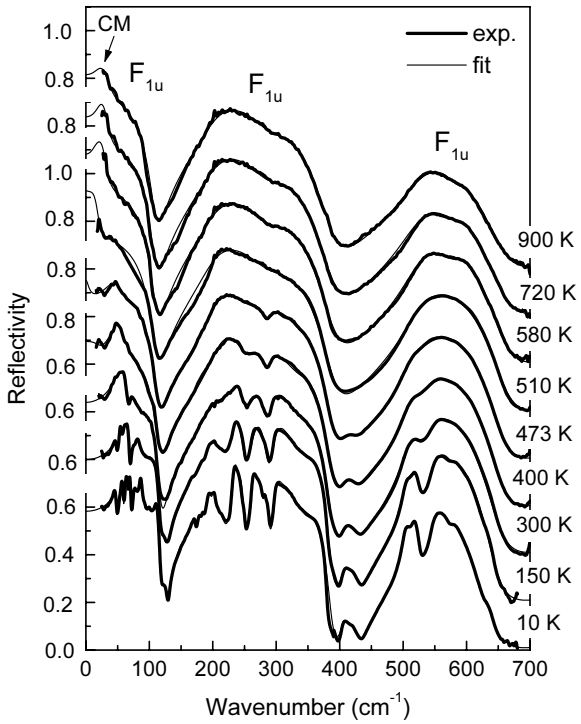

Figure 1. IR reflectivity spectra of PZ ceramics at selected temperatures below and above the antiferroelectric phase transition. Thick lines indicate the experimental data, thin lines the fit.

3. Results and evaluation

Figure 1 shows the reflectivity spectra of the PZ ceramics at selected temperatures. No mode features were seen above the shown frequency range. Since the grains of the investigated ceramics were only a few μm large, we could consider our sample as homogeneous compared to the IR wavelength and the tensorial components of the dielectric function as averaged in the volume neglecting the very small porosity (effective medium approximation). The spectra were fitted (see thinner lines in figure 1) with a generalized four-parameter model, which is known to give the best results in the case of broad reflectivity bands [18]. The factorized form of the dielectric function explored in this model,

$$\varepsilon^*(\omega) = \varepsilon'(\omega) - \mathrm{i}\varepsilon''(\omega) = \varepsilon_\infty \prod_{j=1}^{n} \frac{\omega_{LOj}^2 - \omega^2 + \mathrm{i}\omega\gamma_{LOj}}{\omega_{TOj}^2 - \omega^2 + \mathrm{i}\omega\gamma_{TOj}}$$

is related to the fitted reflectivity via

$$R(\omega) = \left| \frac{\sqrt{\varepsilon^*(\omega)} - 1}{\sqrt{\varepsilon^*(\omega)} + 1} \right|^2 .$$

Here $\varepsilon_\infty = n^2 = 4.8$ [23] is the high frequency optical permittivity, ω_{TOj} and ω_{LOj} denote the transverse and longitudinal eigenfrequencies of the jth polar mode and γ_{TOj} and γ_{LOj} denote their respective damping constants. The dielectric strength of the jth mode is approximately

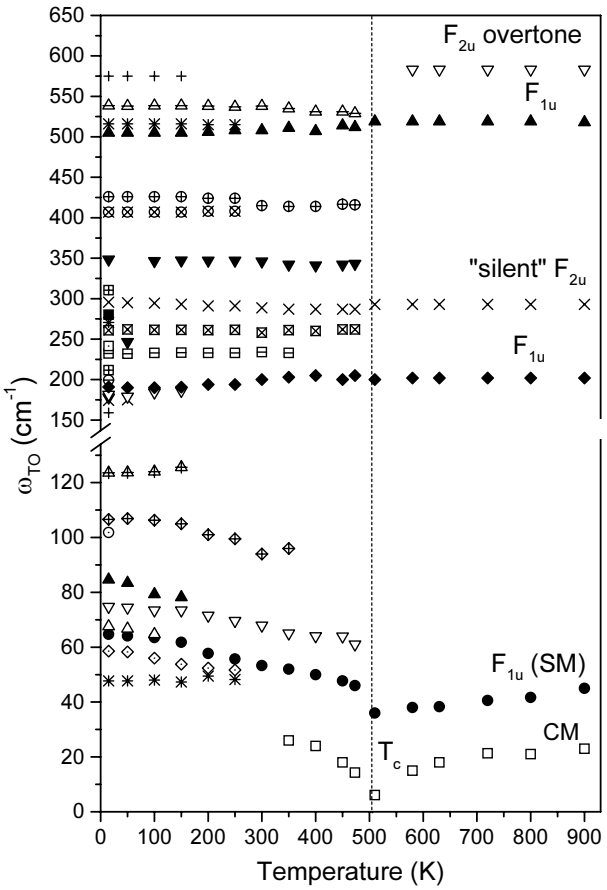

Figure 2. Temperature evolution of the polar transverse mode eigenfrequencies.

given by [18]

$$\Delta\varepsilon_j = \varepsilon_\infty \prod_k (\omega_{LOk}^2 - \omega_{TOj}^2)\left(\omega_{TOj}^2 \prod_{k\neq j} (\omega_{TOk}^2 - \omega_{TOj}^2)\right)^{-1}.$$

The fitting parameters for six selected temperatures are presented in table 2. The temperature dependences of transverse eigenfrequencies of all the fitted modes are plotted in figure 2. At the lowest temperature as many as 30 modes were resolved. On increasing temperature their number gradually decreases. Above room temperature an additional overdamped mode (central mode) was added to the fitting model.

The dielectric response functions obtained by fitting the IR reflectivity spectra at low temperatures (10–300 K) were compared to the data of submillimetre coherent source spectroscopy. They appeared to be in a good agreement (figure 3) and both indicated the decrease of the permittivity on cooling (from $\varepsilon' \sim 80$ at 300 K to 55 at ∼10 K). This effect reflects the slight hardening of low-frequency (50–100 cm^{-1}) polar phonons which may be noticed from figure 2. At room temperature only three of these modes remain distinguishable in the reflectivity spectrum: the strongest one (full circles in figure 2, see also table 2) is the lowest-frequency polar phonon. Its frequency decreases from 65 cm^{-1} at ∼10 K to 53 cm^{-1} at room temperature. On further heating it continues to soften down to ∼36 cm^{-1} at T_c.

Table 2. Fitted mode parameters of PZ ceramics for selected temperatures ($\omega_{TO}, \gamma_{TO}, \omega_{LO}, \gamma_{LO}$ are expressed in cm^{-1}).

~10 K					300 K					473 K				
ω_{TO}	γ_{TO}	ω_{LO}	γ_{LO}	$\Delta\varepsilon$	ω_{TO}	γ_{TO}	ω_{LO}	γ_{LO}	$\Delta\varepsilon$	ω_{TO}	γ_{TO}	ω_{LO}	γ_{LO}	$\Delta\varepsilon$
										14.3	67	18.0	63	79
47.7	4.2	48.6	2.6	3.4										
58.6	2.9	59.3	1.6	2.7										
64.7	6.1	71.2	3.2	7.9	53	25	65	7.4	51	46	39	57	29	82
67.6	4.8	66.0	2.6	6.8										
74.7	8.4	117.9	6.8	6.3	68	11	118	16	3.7	61	55	114	23	18
84.6	6.4	81.5	10	1.9										
101.8	24	89.9	13	4.2	94	43	81	30	6.7					
106.6	9.3	105.0	8.7	1.8										
123.6	13	127.8	8.5	0.6										
159.1	19	159.2	15	0.06										
174.3	15	174.4	7.2	0.2										
177.9	17	221.0	29	6.7	200	44	229	54	10	205	35	247	67	10
181.3	3.2	181.2	2.8	0.2										
190.8	10	186.8	9.3	2.5										
199.3	4.4	198.9	4.8	0.2										
211.6	7.7	211.1	8.2	0.07										
232.3	7.2	250.7	16	1.2	234	31	249	23	1.0					
241.5	9.2	240.0	9.9	0.2										
260.9	10	289.9	12	1.0	258	33	284	19	1.6	261	68	282	23	1.9
270.7	11	269.2	10	0.2										
280.1	7.8	278.7	7.7	0.1										
285.7	11	387.8	19	0.4	289	21	387	24	0.5	285	26	387	35	0.4
310.5	17	309.8	17	0.03										
348.3	81	328.5	75	0.5	346	79	332	74	0.4	341	81	332	79	0.3
406.9	14	409.2	20	0.03										
426.1	33	431.7	20	0.09	415	33	425	30	0.1	417	35	422	34	0.07
505	21	527.5	23	0.9	508	33	528	35	1.0	515	43	527	44	1.1
516.3	10	515.1	11	0.07										
538.5	28	645	44	0.4	538	38	650	52	0.4	531	58	653	49	0.4
574.9	21	574.0	21	0.01										

510 K					580 K					900 K				
ω_{TO}	γ_{TO}	ω_{LO}	γ_{LO}	$\Delta\varepsilon$	ω_{TO}	γ_{TO}	ω_{LO}	γ_{LO}	$\Delta\varepsilon$	ω_{TO}	γ_{TO}	ω_{LO}	γ_{LO}	$\Delta\varepsilon$
6.1	14	20	15	2658	15	16	32	20	914	23	24	35	29	290
36	100	112	26	175	38	100	112	24	81	45	108	110	24	72
200	51	391	50	14	201	53	391	57	14	202	54	389	60	14
293	74	285	71	0.9	293	74	285	71	0.6	293	79	285	73	0.6
519	66	659	53	1.5	519	67	657	57	1.4	519	85	655	67	1.4
					583	46	581	50	0.03	583	53	581	52	0.03

Therefore below we will refer to this mode as the soft mode.

The complex dielectric response obtained by fitting the room temperature IR spectrum is shown in figure 4. The fitting curve is in a good agreement with the terahertz, submillimetre and microwave data obtained on the same sample and with the microwave data on the other PZ ceramics [8–10]. It speaks in favour of the purely phonon contribution to the submillimetre and microwave value of the room temperature permittivity as well as the appreciable reliability of the present IR data and their fit.

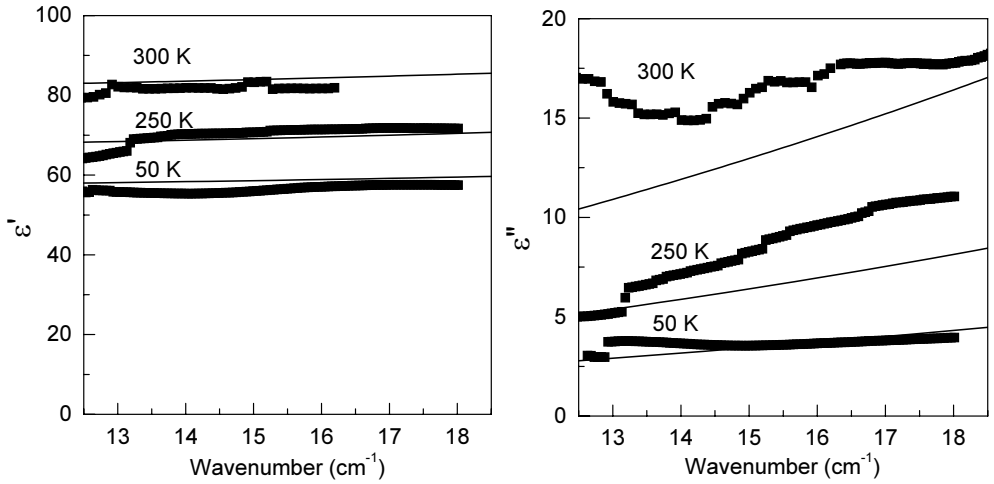

Figure 3. Real and imaginary part of the dielectric function at selected temperatures obtained from the fit to IR reflectivity spectra in comparison with the experimental data of coherent source submillimetre spectroscopy.

On approaching T_c, in spite of a partial softening of the lowest-frequency mode, the permittivity value measured at 36 GHz starts to exceed the total contribution of all IR phonons $\Delta\varepsilon_{ph}$ (figure 5). This fact indicates the presence of another dispersion source in the GHz–THz range, which becomes rather strong to be neglected near and above T_c. Hence, starting from 350 K we included in our fitting model an extra mode, overdamped and lying at lower frequencies than those of phonons, and assigned it as the central mode. Nevertheless, it should be pointed out that in the antiferroelectric phase the central mode is not seen directly in our far IR spectra and thus its parameters cannot be determined accurately.

Just above T_c, the low-frequency reflectivity (below 50 cm^{-1}) becomes strongly enhanced. On further heating, this area is extended to higher frequencies and the effect is much more clearly observable in far IR spectra. Comparing these data with the reflectivity of the PZ single crystal [13], where a clear maximum was observed above T_c in the same frequency range, we can conclude that a similar fitting model is applicable. The increase in reflectivity and its spreading to higher frequencies can be interpreted as hardening of two modes: one from 6 to 23 cm^{-1} and another from 36 to 45 cm^{-1}. We assigned them to the previously introduced central and soft mode respectively. Due to the high permittivity we failed to perform the microwave measurements above 500 K. However, our fit, where the central mode was added to the polar phonons, allowed us to achieve quite good agreement with the microwave data by Poplavko and Tsykalov [8, 9]. It should be taken into account that above T_c the estimated 3% accuracy of the low-frequency end of IR reflectivity results in ∼40% error in the dielectric permittivity in the GHz–THz range and in rather low accuracy of the soft and central mode fit parameters. This limited accuracy did not allow us to perform analysis of the possible coupling between both modes [24].

4. Discussion

4.1. Mode assignment

In the cubic phase the factor-group analysis for the vibrational representation yields $\Gamma_{vibr} = 4F_{1u} + 1F_{2u}$. Three F_{1u} modes are expected to be IR active and one corresponds to the acoustic

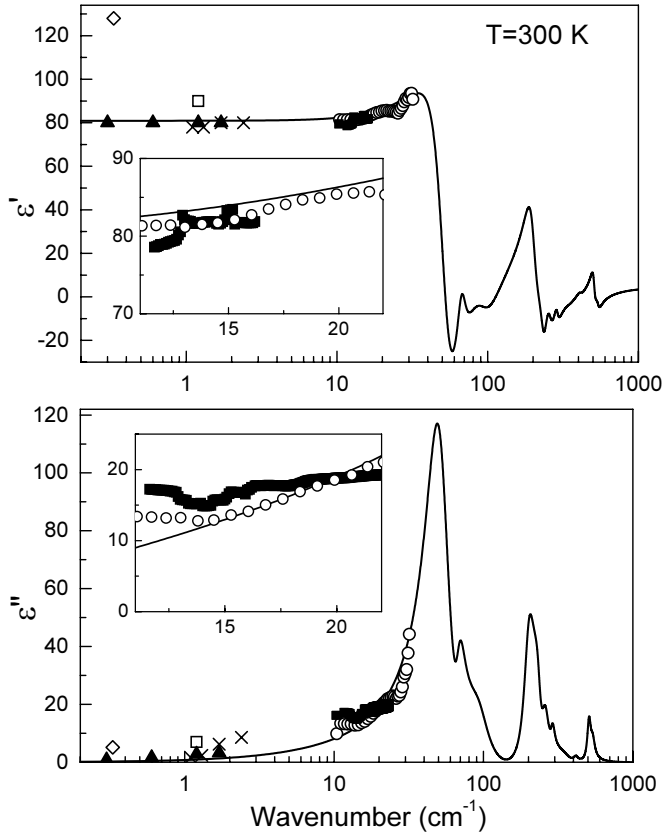

Figure 4. Room temperature spectra of the real and imaginary part of the dielectric function: lines—result of the fit; full squares—data of the coherent source submillimetre spectroscopy; open circles—data of the time-domain terahertz transmission spectroscopy; open squares—microwave data of the present work; full triangles, crosses and open diamonds—data obtained by other authors [8],[9] and [10] respectively.

triplet. The F_{2u} triplet is silent. In the orthorhombic antiferroelectric phase, the factor-group analysis on the basis of structural data [1] yields [25]

$$\Gamma_{vibr} = 16\mathrm{Ag} + 12\mathrm{Au} + 16\mathrm{B}_{1g} + 12\mathrm{B}_{1u} + 14\mathrm{B}_{2g} + 18\mathrm{B}_{2u} + 14\mathrm{B}_{3g} + 18\mathrm{B}_{3u}$$

predicting 45 polar modes in the IR spectra of polycrystalline PZ samples.

The number of modes evaluated by fitting the IR reflectivity spectra (see figure 2 and table 2) at low temperatures is somewhat lower (30) than predicted. This can be explained by mode overlapping that does not allow us to resolve all of them. The decrease in the number of resolved modes on heating is a typical manifestation of the increase in the mode dampings. At room temperature we can still resolve as many as 11 modes, which is significantly more than seen by Perry *et al* [12]. Nevertheless, our main spectral features correspond to their results. If we consider the whole low-frequency reflectivity band (10–120 cm^{-1}), which includes the soft mode as a single band without resolving the individual modes (pseudocubic approximation), its contribution to static permittivity amounts to ∼90% as in [12]. However, our fit gives somewhat lower low-frequency permittivity $\varepsilon' \sim 80$ compared to [12] ($\varepsilon' \sim 120$).

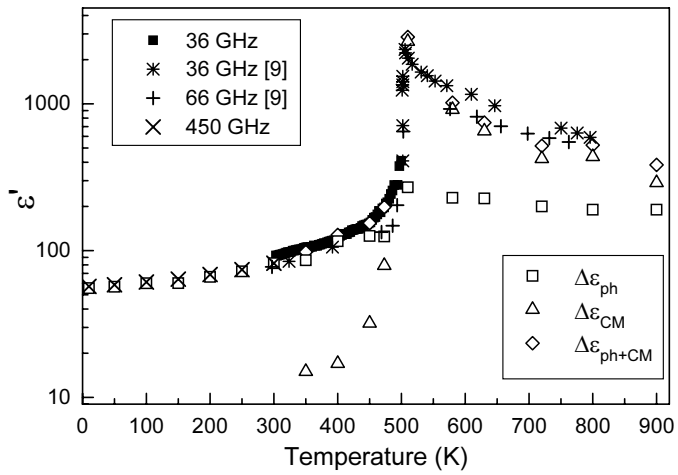

Figure 5. Temperature dependence of the summarized dielectric strength of all polar phonons $\Delta\varepsilon_{ph}$, strength of the central mode $\Delta\varepsilon_{CM}$ and total IR permittivity $\Delta\varepsilon_{ph+CM}$ in comparison with our low-temperature submillimetre (∼450 GHz), microwave (36 GHz) data and microwave data from [9].

Above T_c we see three broad, well distinguishable phonon bands in accordance with the factor group analysis. Following the usual assignment [12] they can be regarded as the F_{1u} modes: the lowest-frequency one corresponds mainly to Pb–ZrO_6 vibrations, the middle to O–Zr–O bending and the highest to Zr–O stretching vibration. The lowest-frequency mode is called here the soft mode even though it is clear that the critical soft mode lies outside the Brillouin zone centre and is not IR active. Our IR-active soft mode, however, may contribute to the sharp dielectric anomaly at T_c, which might be connected with its partial softening. Our fit actually indicates its softening from ∼45 cm^{-1} at 900 K to 36 cm^{-1} near T_c. Its high damping constant (∼100) in the paraelectric prevents us, however, from determining the eigenfrequency accurately.

One comment on the 'critical' antiferroelectric soft mode outside the Brillouin zone centre. The group analysis of the antiferroelectric phase transition shows that at least two different order parameters (at the R(111) and $\Sigma(1/4\,1/4\,0)$ points of the Brillouin zone) are necessary to explain the symmetry lowering and unit cell multiplicity (eight times) [26]. As no inelastic neutron scattering data are available, it is not clear which of the order parameters (soft modes) is the primary one and which is triggered by the primary parameter. Nevertheless, from the sharp (almost divergent) dielectric anomaly and the first-order nature of the transition it follows that also the ferroelectric instability at the $\Gamma(000)$-point must be nearly as pronounced as the antiferroelectric ones. This helps to understand that the appearance of the intermediate ferroelectric phase could be a quite delicate question.

As already mentioned, besides the lattice modes predicted by the factor-group analysis, we included in our fit near and above T_c also one low-frequency overdamped excitation—the central mode. We assigned it to a dynamical disorder of the lattice (particularly anharmonic Pb atom hopping, see later), which might be quite pronounced in the paraelectric phase. Another evidence for the lattice disorder may be seen from the asymmetry of the middle band above T_c (see figure 1). In spite of the selection rules, which predict three IR active modes in the paraelectric phase, the shape of the middle band cannot by fitted by only one mode. In order to achieve good agreement with the experimental curves we added to the fit one extra mode lying near 290 cm^{-1}, weak and heavily damped. Its frequency corresponds to the 'silent' F_{2u}

mode [12, 27, 28], which can become active owing to the local cubic symmetry breaking due to strong dynamic fluctuations. On further heating a similar weak mode is observed in our IR reflectivity spectra at the doubled frequency of ∼580 cm^{-1}. It can be assigned to a two-phonon process, strengthening with increasing temperature. It is interesting to note that the frequency of our soft mode in the paraelectric phase corresponds to that obtained from the fit of the defect induced Raman spectra [16], though in the later paper [17] higher values were reported.

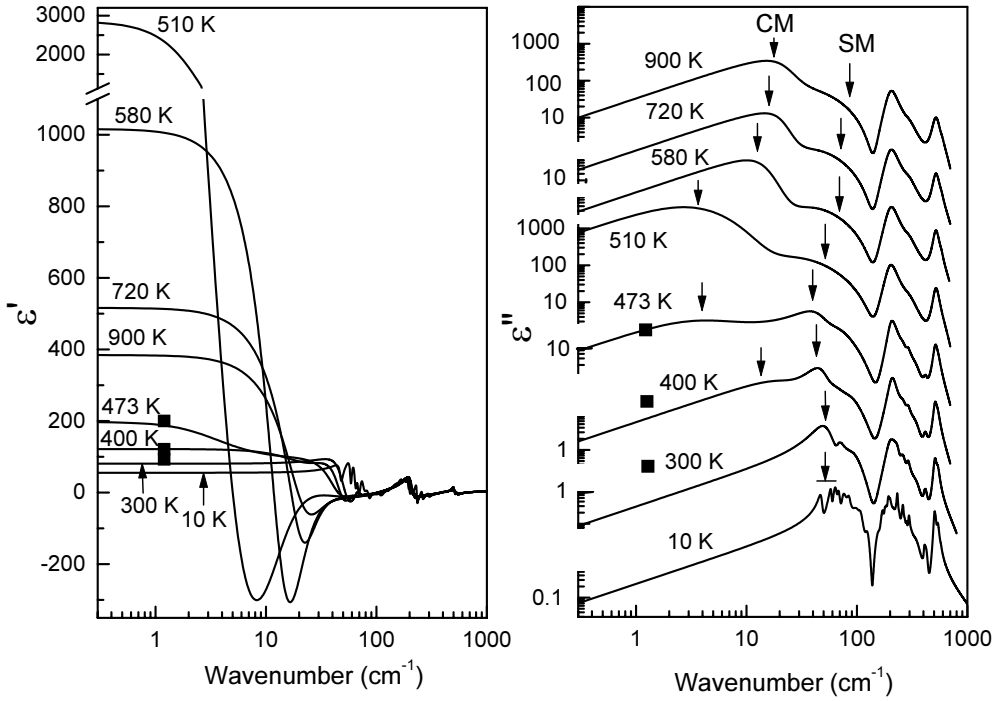

Figure 6. Real and imaginary parts of the dielectric function at selected temperatures, obtained from the fit to IR reflectivity spectra. Full squares indicate the microwave data at 36 GHz.

4.2. Dielectric function

Real and imaginary parts of the dielectric function at selected temperatures are plotted in figure 6. The summarized dielectric strength of all polar phonons $\Delta\varepsilon_{ph}$, the strength of the central mode $\Delta\varepsilon_{CM}$ as well as the total IR permittivity $\Delta\varepsilon_{ph+CM}$ are plotted as functions of temperature in figure 5. In order to estimate the contribution of these high-frequency dispersion mechanisms to the static permittivity we added to figure 5 the data at 36 GHz and in the submillimetre range (∼450 GHz). The only available microwave data for the paraelectric phase were taken from [9]. From the lowest to room temperature, the permittivity in the GHz region can be completely explained by the phonon contribution. At higher temperatures up to T_c the lattice contribution remains dominating but not sufficient. Above T_c, it becomes only a weak part (<10% at T_c) of the GHz permittivity. In this case the mode softening is not sufficient to describe the dielectric anomaly at the phase transition, and the central mode contribution $\Delta\varepsilon_{SM}$ is needed to fit the microwave values. It characterizes the central mode as the dispersion mechanism which dominates in the paraelectric phase and is responsible for most of the dielectric anomaly.

4.3. Nature of the antiferroelectric transition

In figure 6 we plotted temperature evolution of the complex dielectric function and marked positions of the central and soft mode in the loss spectrum by arrows. While far below T_c the soft mode dominates the spectrum and weakly softens towards the phase transition, in the paraelectric phase its role is taken over by the lower frequency central mode. Such a behaviour represents a typical example of mixed displacive and order–disorder regimes near a structural phase transitions: the soft mode characterizes the former and the central mode the latter one.

The order–disorder features of the phase transition are accounted for by the lattice disorder that is also responsible for other anharmonic effects observed in the paraelectric phase in our IR spectra. Its microscopic origin most probably lies in highly anharmonic Pb hopping [6, 13]. This assumption is strongly supported by recent reports on the Pb-containing relaxor perovskite ferroelectrics: $PbMg_{1/3}Nb_{2/3}O_3$ (PMN), $PbMg_{1/3}Ta_{2/3}O_3$ (PMT) and $PbSc_{1/3}Ta_{2/3}O_3$ (PST) [29–31], where the appearance of a central mode is attributed to the local lead disorder.

The order–disorder character of the antiferroelectric phase transition in Pb-based perovskites has been indicated in [32] based on a transmission electron microscopy study, where the diffuse superlattice reflections, assigned to locally ordered polar clusters, have been observed at temperatures far above the antiferroelectric transformation. On the basis of the pair-distribution function analysis with pulsed neutron powder diffraction measurements it was also found [33] that in PMN, PMT–PZ, PZT and PZ, regardless of local chemistry, Pb ions distort the environment of the oxygen neighbours, become off-centred and exhibit therefore local dipole moments.

First principles computations using variational density-functional perturbation theory also confirm the important role of the Pb ions in the lattice dynamics of perovskites with the general formula ABO_3 [34, 35]. It turns out that Pb strongly strengthens the A–O coupling (e.g. in comparison with Ba), which is directly responsible both for the involvement of Pb in the ferroelectric soft mode eigenvector and the appearance of the antiferrodistortive instability. It has been also suggested [34] that the presence of entire branches of unstable phonons in the Pb subspace may cause local polar distortions above T_c.

Not to omit the still speculative question on the intermediate ferroelectric phase, we would like to mention that, according to the temperature dependence of the permittivity, measured on a similar ceramic sample in the kHz–MHz range [7], this intermediate phase is probably not present in our sample. The accuracy of the present IR experiment did not allow us to draw conclusions about its presence, nor about the questionable weak polar symmetry of the antiferroelectric phase [11].

5. Conclusions

We have performed a detailed analysis of the dielectric response of PZ ceramics as a function of frequency and temperature in the 10^{10}–10^{12} Hz range where the discrepancy in the data, reported by different authors, caused a controversial interpretation of the antiferroelectric phase transition nature. In order to achieve the most objective conclusions we took into consideration not only our infrared, submillimetre, terahertz and microwave data but all other results in this frequency range we were aware of. This enabled us to determine the role of the lattice vibrations in the antiferroelectric phase transition and estimate the parameters of the central mode, playing an important role in this transition. Though our work confirms the mixed displacive and order–

disorder nature of the phase transition suggested in [6] and [17], we found the central mode at much higher frequencies of ∼5–25 cm^{-1} than in [6] and [17].

We determined the temperature dependence of the long-wavelength polar optical mode parameters. In the paraelectric phase we assigned the modes in accordance with the factor-group analysis and first-principles calculations, and brought evidence of the strong lattice anharmonicity above T_c.

Acknowledgments

The authors are grateful to K Roleder and J Dec for their helpful discussion. One of us (AP) is indebted to the 1. Physikalisches Institut, Universität Stuttgart for the hospitality and financial support of his stay in Germany. The work was supported by the Grant Agency of the Czech Republic (project No 202/98/1282 and 202/01/0612), the Grant Agency of the AS CR (project Nos A1010828 and A1010918), the Ministry of Education of the Czech Republic (project COST OC 525.20) and by the Deutsche Forschungsgemeinschaft (DFG) via GO 976/1-1.

References

[1] Fujishita H, Shiozaki Y, Achiva A and Sawaguchi E 1982 *J. Phys. Soc. Japan* **51** 3583
[2] Corker D L, Glazer A M, Dec J, Roleder K and Whatmore R W 1997 *Acta Crystallogr.* B **53** 135
[3] Ujma Z and Handerek J 1983 *Phase Transitions* **3** 121
[4] Ujma Z 1984 *Phase Transitions* **4** 169
[5] Roleder K and Dec J 1989 *J. Phys.: Condens. Matter* **1** 1503
[6] Roleder K, Maglione M, Fontana M D and Dec J 1996 *J. Phys.: Condens. Matter* **8** 10 669
[7] Nokhrin S N, Laguta V V, Glinchuk M D, Bykov I P, Lyaschenko A B, Jastrabik L, Wanzong Y, Jianrong Z and Gaomin L 1998 *J. Kor. Phys. Soc.* **32** S308
[8] Poplavko Yu M and Tsykalov V G 1967 *Fiz. Tverd. Tela.* **9** 3305 (in Russian)
[9] Tsykalov V G and Poplavko Yu M 1970 *Izvest. Akad. Nauk SSSR* **34** 2586 (in Russian)
[10] Lanagan M T, Kim J H, Jang S-J and Newnham R E 1988 *J. Am. Ceram. Soc.* **71** 311
[11] Dai X, Li J-F and Viehland D 1995 *Phys. Rev.* B **51** 2651
[12] Perry C H, McCarthy D J and Rupprecht G 1965 *Phys. Rev.* **138** A1537
[13] Ostapchuk T, Petzelt J, Zelezny V, Kamba S, Malic B, Kosec M, Cakare L, Roleder K and Dec J 2000 *Ferroelectrics* **239** 109
[14] Pasto A E and Condrate R A 1973 *J. Am. Ceram. Soc.* **56** 436
[15] Roleder K, Kugel G E, Fontana M D, Handerek J, Lahlou S and Carabatos-Nedelec C 1989 *J. Phys.: Condens. Matter* **1** 2257
[16] Jankowska-Sumara I, Kugel G E, Roleder K and Dec J 1996 *Ferroelectrics* **185** 169
[17] Roleder K, Jankowska-Sumara I, Kugel G E, Maglione M, Fontana M D and Dec J 2000 *Phase Transitions* **71** 287
[18] Gervais F 1983 *Infrared and Millimeter Waves* vol 8, ed K J Button (New York: Academic) p 279
[19] Kozlov G and Volkov A 1998 *Millimeter and Submillimeter Wave Spectroscopy of Solids* ed G Gruner (Berlin: Springer) p 51
[20] Kuzel P and Petzelt J 2000 *Ferroelectrics* **239** 79
[21] Hippel A (ed) 1954 *Dielectric Materials and Applications* (London: Chapman and Hall)
[22] Grigas J 1996 *Microwave Dielectric Spectroscopy of Ferroelectrics and Related Materials* (Amsterdam: GB)
[23] Jona F, Shirane G and Pepinsky R 1954 *Phys. Rev.* **97** 1584
[24] Petzelt J, Kozlov G V and Volkov A A 1987 *Ferroelectrics* **73** 101
[25] Pokorny J, Petzelt J, Gregora I, Zelezny V, Vorlicek V, Zikmund Z, Fedorov I, Pronin A and Kosec M 1996 *Ferroelectrics* **186** 115
[26] Fujishita H and Hoshino S 1984 *J. Phys. Soc. Japan* **53** 226
[27] Zelezny V, Simon P, Gervais F and Kela T 1987 *Mater. Res. Bull.* **22** 1695
[28] Petzelt J *et al* 2000 *Integrated Ferroelectrics* at press

[29] Petzelt J, Buixaderas E and Pronin A V 1998 *Mater. Sci. Eng.* B **55** 86
[30] Bovtun V, Porokhonskyy V, Petzelt J, Savinov M, Endal J, Ellisalde C and Malibert Ch 2000 *Ferroelectrics* **238** 17
[31] Naberezhnov A, Vakhrushev S, Dorner B, Strauch D and Moudden H 1999 *Eur. Phys. J.* B **11** 13
[32] Viehland D 1995 *Phys. Rev.* B **52** 778
[33] Egami T, Teslic S, Dmowski W, Davies P K, Chen I-W and Chen H 1998 *J. Kor. Phys. Soc.* **32** S935
[34] Waghmare U V and Rabe K M 1997 *Ferroelectrics* **194** 135
[35] Ghosez Ph, Cockayne E, Waghmare U V and Rabe K M 1999 *Phys. Rev.* B **60** 836